First-Principles Calculation of Optical Properties of C_{60} in the fcc Lattice

W. Y. Ching, Ming-Zhu Huang, and Yong-Nian Xu
Department of Physics, University of Missouri-Kansas City, Kansas City, Missouri 64110

W. G. Harter and F. T. Chan
Department of Physics, University of Arkansas, Fayetteville, Arkansas 72701
(Received 12 July 1991)

The electronic and optical properties of C_{60} in the fcc lattice have been studied by a first-principles method. It is shown that C_{60} has a low dielectric constant and an optical spectrum rich in structures; this is drastically different from diamond and graphite. The spectrum shows five disconnected absorption bands in the 1.4 to 7.0 eV region with sharp structures in each band that can be attributed to critical-point transitions. This is a manifestation of the localized molecular structure coupled with long-range crystalline order.

PACS numbers: 78.20.Bh, 71.25.Tn

The recent discovery of the third form of carbon in the form of C_{60} fullerene [1] and its crystalline form with a fcc lattice [2] has prompted an upsurge of experimental and theoretical studies [3–11]. Research efforts were further accelerated by the announcement of the fact that when intercalated with alkali elements such as K [12–14] and Rb [15], the C_{60} crystal becomes superconducting with a T_c approaching 28 K [15]. Therefore, it is extremely important to understand the fundamental electronic properties of this fascinating material. In this paper we report a first-principles calculation of the electronic and optical properties of C_{60} in the fcc lattice. Although a number of theoretical calculations on isolated C_{60} clusters exist (see references cited in [4]), the study of the optical properties of the C_{60} crystal is especially important. The unique structure of C_{60} in the crystalline form raises the question of the proper interplay of the localized molecular structure and the long-range periodicity in the determination of the electron wave function.

We have used the first-principles, self-consistent, orthogonalized linear combination of atomic orbitals (OLCAO) method in the local-density approximation to calculate the electronic structure of fcc C_{60}. The Wigner interpolation formula was employed for the correlation correction. This method has been widely used in the study of band structures and optical properties of a large number of solids, especially those with complex structures [16]. The method is uniquely suited for C_{60} since even with a simple fcc structure, the unit cell contains 240 valence electrons and an economic expansion in the basis function is crucial [17]. The fcc lattice constant used was 14.20 Å with two types of C-C bonds (1.46 and 1.40 Å) in the icosahedral C_{60} cluster. The relative orientation of the C_{60} cluster with respect to the z axis was chosen to be the same as that in Ref. [7]. The basis functions were Bloch functions which are linear combinations of atomic C $1s$, $2s$, and $2p$ orbitals. The atomic orbitals were expressed as combinations of sixteen Gaussian-type orbitals with decaying exponents ranging from 50000 to 0.15. A high degree of accuracy in fitting the electron charge distribution as a sum of atom-centered Gaussian functionals has been achieved [16]. Because of the large unit cell, only two special k points were used in the self-consistent cycle, while for the density-of-states (DOS) calculation, 89 k points in the irreducible portion of the fcc Brillouin zone (BZ) were employed. The large degree of k-point sampling in the BZ in conjunction with the linear analytic tetrahedron method enabled us to evaluate the DOS with high precision without using the Gaussian broadening procedure which may wash out van Hove singularities. For the optical calculation, we have limited the transition frequency to within the 10 eV range, i.e., all interband transitions from 10 eV below the top of the occupied valence band (VB) to 10 eV above are included. All relevant dipole matrix elements associated with each pair of transitions at each k point were included using the wave functions obtained from the band calculation. Symmetry-forbidden transitions were automatically excluded by having zero transition matrix elements between the Bloch states.

Figure 1 shows the calculated band structure near the gap. This band structure is similar to the work of Ref.

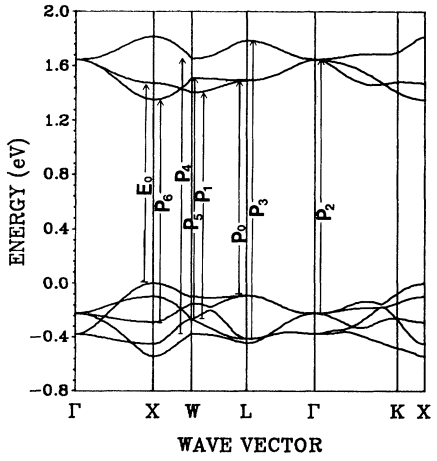

FIG. 1. Calculated band structure of C_{60} in the fcc lattice near the gap. Arrows show critical-point transitions.

[7] with the exception of some different ordering in energy at the X point. We obtained direct band gaps of 1.34 eV at X and 1.87 eV at Γ. This difference of about 0.5 eV may represent the difference in the gap value between a cluster calculation and the present band calculation. Since the local-density theory generally underestimates the band gap of an insulator, it is conceivable that the true gap may be somewhat larger. A similar calculation for diamond gives an indirect band gap of 4.54 eV compared to the experimental value of 5.47 eV. The bandwidths of the top VB and the first set of unoccupied conduction bands (CB) are 0.55 and 0.54 eV, respectively. The averaged electron and hole effective masses at X are estimated to be $1.45m$ and $1.17m$, respectively.

The high-resolution DOS spectrum from -6 to $+6$ eV is shown in Fig. 2. In this region, the VB and the CB can be roughly characterized as having five major pieces each (labeled $V1$, $V2$, $V3$, $V4$, and $V5$ and $C1$, $C2$, $C3$, $C4$, and $C5$, respectively). The bandwidths for each piece range from 0.5 to 1.0 eV. The considerable band dispersion implies that it is not adequate to approximate the electronic structure of a fcc C_{60} with that of an isolated C_{60} cluster. However, the narrow bands with minigaps do originate from the rather flat molecular crystal-like band structures. For example, $V5$ actually consists of two separate pieces with a gap of 0.11 eV. The calculated DOS is in good agreement with the photoemission data from Refs. [4,12] and also with other recent calculations [4,6,7].

The calculated real and imaginary parts of the dielectric function and the energy-loss function are shown in Figs. 3(a)–3(c). The results of Fig. 3 can be summarized as follows: (1) The optical spectrum of fcc C_{60} is very rich in structure. The absorption intensity decreases with increasing photon energy with no noticeable absorption beyond 7 eV. (2) Broadly speaking, the spectrum consists of five major structures (labeled A, B, C, D, and E) centered at 1.8, 2.7, 4.3, 5.3, and 6.3 eV, respectively. Each absorption band has many sharp substructures. It is easy to assign these transitions as arising from the occupied to the unoccupied localized bands shown in Fig. 2 as follows: A, $V1\rightarrow C1$; B, $V1\rightarrow C2$ and $V2\rightarrow C1$; C, $V1\rightarrow C3$ and $V2\rightarrow C2$; D, $V2\rightarrow C3$ and $V1\rightarrow C4$; E, $V1\rightarrow C5$ and $V2\rightarrow C4$. We shall return later to the discussion of specific transitions in the structure A near the threshold. In the inset of Fig. 3(a), we compare the calculated conductivity $\sigma(\omega)=(\omega/4\pi)\varepsilon_2(\omega)$ with the visible-ultraviolet absorption spectrum of solid C_{60} on quartz [3] in arbitrary units without any shift in wavelength. Peaks C and D agree with the data well. Peak B appears as a weak plateau in the data. The measured peak at 339 nm is absent in the calculated curve and could possibly come from the presence of C_{70}. (3) The real part of the dielectric function $\varepsilon_1(\omega)$ is obtained from the imaginary part $\varepsilon_2(\omega)$ through the Kramers-Kronig transformation. The static dielectric constant ε_0 or $\varepsilon_1(0)$ of 4.4 is low and comparable to that of diamond, but is much smaller than that of Si or GaAs with similar gap sizes. (4) The energy-loss function ($=\mathrm{Im}[-1/\varepsilon(\omega)]$) for fcc C_{60} is

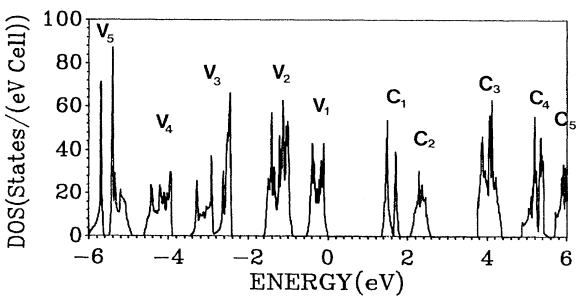

FIG. 2. Calculated DOS of fcc C_{60}. Zero energy at the top of VB.

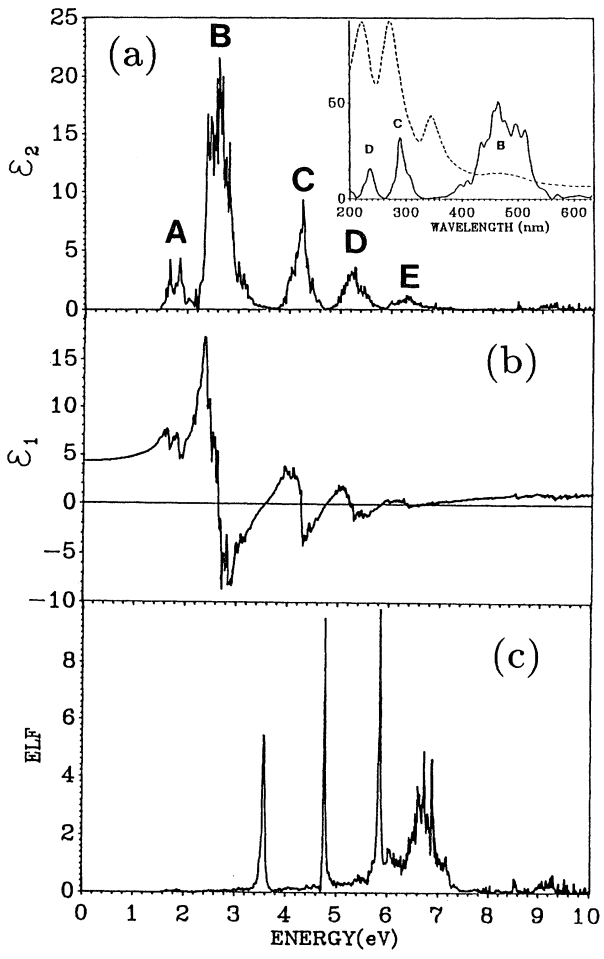

FIG. 3. Calculated (a) imaginary part of the dielectric function, (b) real part of the dielectric function, and (c) energy-loss function. Inset: Calculated conductivity curve (solid line) compared with the visible-ultraviolet absorption spectra from Ref. [3] (dashed line) in arbitrary units.

shown in Fig. 3(c). There are three very sharp structures at 3.5, 4.8, and 5.8 eV corresponding to the energy locations where $\varepsilon(\omega)$ vanishes. A broader peak centered at 6.7 eV is also evident. This peak can be fitted by a Gaussian form with a full width at half maximum of 0.5 eV. This broad peak may come from a collective excitation of the shelled electronic charges of the icosahedral cage. Such structures in the energy-loss function can be measured by the inelastic electron-scattering technique [18].

We now return to discuss the optical absorption within 2 eV of the threshold and defer the discussion for other regions to future publication. The enlarged $\varepsilon_2(\omega)$ curve for this region is shown in Fig. 4. Transitions in this region are from the top set of VB near the gap to the first set of unoccupied CB shown in Fig. 1. The $\varepsilon_2(\omega)$ curve shows the transition threshold to be at 1.46 eV, larger than the minimum direct gap of 1.34 eV at X. This is because the transition from the top of VB to the bottom of CB at X is symmetry forbidden as already pointed out in Ref. [7]. The transition threshold E_0 appears to be from the top of VB to the second CB at X. This is similar to the case in the Cu_2O crystal [19], except in Cu_2O the minimum transition occurs at the zone center. One might expect that some transitions at other **k** points away from X would be allowed, such that the threshold may be at an energy between E_g and E_0. Such was not the case because the dipole matrix elements for transitions in the vicinity of X are all vanishingly small. The small band gap, a similar symmetry-forbidden direct transition as in Cu_2O, leads to the speculation that an exciton may form at X in fcc C_{60} as in Cu_2O. The other structures in Fig. 4 can also be assigned to specific critical-point transitions. For example, the major structures $P1$, $P2$, and $P3$ at 1.67, 1.87, and 2.17 eV can be traced to direct interband transitions at the W, Γ, and L points, respectively. Other smaller structures (P_0, P_6, P_5, and P_4) at 1.6, 1.65, 1.78, and 2.03 eV can be similarly identified as arising from critical-point transitions. These critical-point transitions and the threshold are marked by arrows in the band diagram of Fig. 1. The sharpness of optical transitions in fcc C_{60} is the result of the unique combination of a molecular cluster structure in C_{60}, which gives rise to the localized bands, and the long-range fcc lattice, which gives the critical points in the BZ.

It is of high interest to compare the optical dielectric function of fcc C_{60} with those of the other two forms of carbon, diamond and graphite. Diamond is an insulator with a measured optical gap of 5.7 eV while graphite is a semimetal with a zero gap. In Fig. 5, we show the ε_2 curves of diamond and graphite (in the $\parallel$ and $\perp$ directions) calculated by the same OLCAO method for photon frequency up to 25 eV. It is clear that there is no resemblance with C_{60} whatsoever. In diamond, the single wide absorption band in ε_2 is at 12.0 eV with a maximum only slightly lower than that in C_{60}. For graphite, the absorption is much weaker. In the $\parallel$ direction, the absorption is in the 11 to 16 eV region while in the $\perp$ direction (x-y plane), the absorptions are below 6 eV or above 12 eV. In C_{60}, there is virtually no absorption above 7 eV.

In summary, we have presented the first detailed optical calculation of C_{60} in the fcc lattice which shows a spectacular pattern of structures that can be analyzed in terms of the calculated band structure. It is pointed out that a direct minimal-gap transition at X is symmetry forbidden and the threshold comes from the transition to the second CB, similar to Cu_2O. All the structures in the ε_2 spectrum can be assigned to critical-point transitions

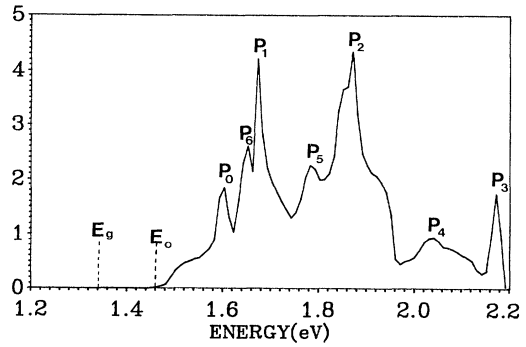

FIG. 4. Imaginary part of the dielectric function of fcc C_{60} near the threshold. E_0 is the transition threshold. P_0–P_6 are critical-point transitions marked in Fig. 1.

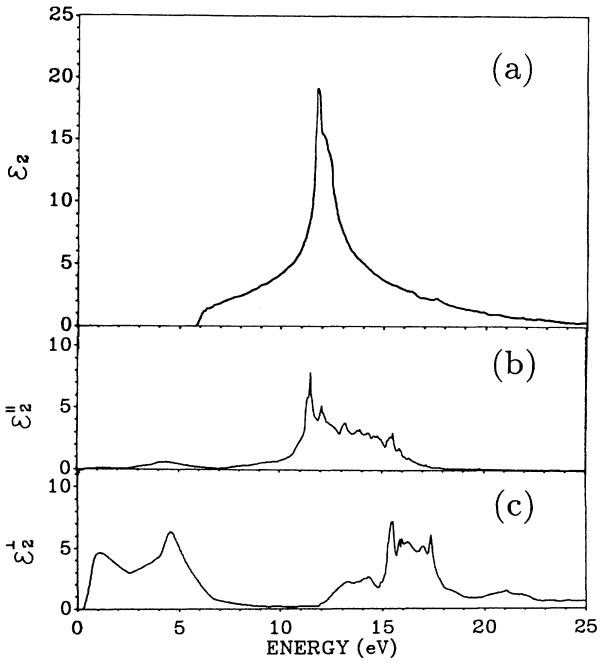

FIG. 5. Imaginary parts of the dielectric function of (a) diamond, (b) graphite in the $\parallel$ direction, and (c) graphite in the $\perp$ direction, calculated by the same OLCAO method.

superimposed on broad band-to-band transitions. Since C_{60} may exist in other crystalline forms [10], or may be doped with alkali or halogen elements that may result in different crystals with different band structures and optical properties, fundamental research along these lines may lead to important applications for C_{60} as a useful optical material. We are currently investigating the effects of pressure on the optical properties of the C_{60} crystal [20] and are performing similar calculations for the C_{60}:K_x system with x varying from 1 to 6 [21]. Preliminary results on C_{60}:K_x indicate the formation of a partially occupied metallic band within an enlarged semiconductor gap. These and other results will be reported later.

This work is supported by the U.S. Department of Energy under Grant No. DE-FG02-84ER45170.

Note added.—Since the submission of this Letter, we became aware of the high-electron-energy-loss spectroscopy measurement of Sohmen, Fink, and Kratschmer [22]. Their data are in excellent agreement with our calculated result of Fig. 3(c). Also, a recent band-structure calculation by Troullier and Martins [23] using pseudopotential method shows the band ordering at X to be the same as ours and different from Ref. [7].

[1] H. W. Kroto, J. R. Heath, S. C. O'Brien, R. F. Curl, and R. E. Smalley, Nature (London) **318**, 162 (1985).
[2] R. M. Fleming *et al.*, Mater. Res. Soc. Symp. Proc. (to be published).
[3] W. Kratschmer, L. D. Lamb, K. Fostiropoulos, and D. R. Huffman, Nature (London) **347**, 354 (1990).
[4] J. H. Weaver *et al.*, Phys. Rev. Lett. **66**, 1741 (1991).
[5] D. L. Lichtenburger *et al.*, Chem. Phys. Lett. **176**, 203 (1991).
[6] Q.-M. Zhang, Jae-Yel Yi, and J. Bernholc, Phys. Rev. Lett. **66**, 2633 (1991).
[7] S. Saito and A. Oshiyama, Phys. Rev. Lett. **66**, 2637 (1991).
[8] P. J. Benning, J. L. Martin, J. H. Weaver, L. P. F. Chibante, and R. E. Smalley, Science **252**, 1417 (1991).
[9] J. E. Fisher *et al.*, Science **252**, 1288 (1991).
[10] P. A. Heiney *et al.*, Phys. Rev. Lett. **66**, 2911 (1991).
[11] R. A. Cappelletti *et al.*, Phys. Rev. Lett. **66**, 3261 (1991).
[12] A. F. Hebard *et al.*, Nature (London) **350**, 600 (1991).
[13] G. K. Wertheim *et al.*, Science **252**, 1419 (1991).
[14] G. Sparn *et al.*, Science **252**, 1829 (1991).
[15] M. J. Rosseninsky *et al.*, Phys. Rev. Lett. **66**, 2830 (1991).
[16] W. Y. Ching, J. Am. Ceram. Soc. **73**, 3135 (1990).
[17] It takes approximately 6 h of CPU time on the local VAX6000 model 540 computer to obtain the self-consistent potential for the fcc C_{60}, an additional 16 h to calculate the DOS and band structures, and another 30 h for the optical properties.
[18] C. Tarrio and S. E. Schnatterly, Phys. Rev. B **40**, 7852 (1989).
[19] W. Y. Ching, Y.-N. Xu, and K. W. Wong, Phys. Rev. B **40**, 8111 (1989).
[20] M.-Z. Huang, Y.-N. Xu, and W. Y. Ching (to be published).
[21] Y.-N. Xu, M.-Z. Huang, and W. Y. Ching (to be published).
[22] E. Sohmen, J. Fink, and W. Kratschmer, Europhys. Lett. (to be published).
[23] N. Troullier and J. L. Martins (to be published).